Supplemental Figures

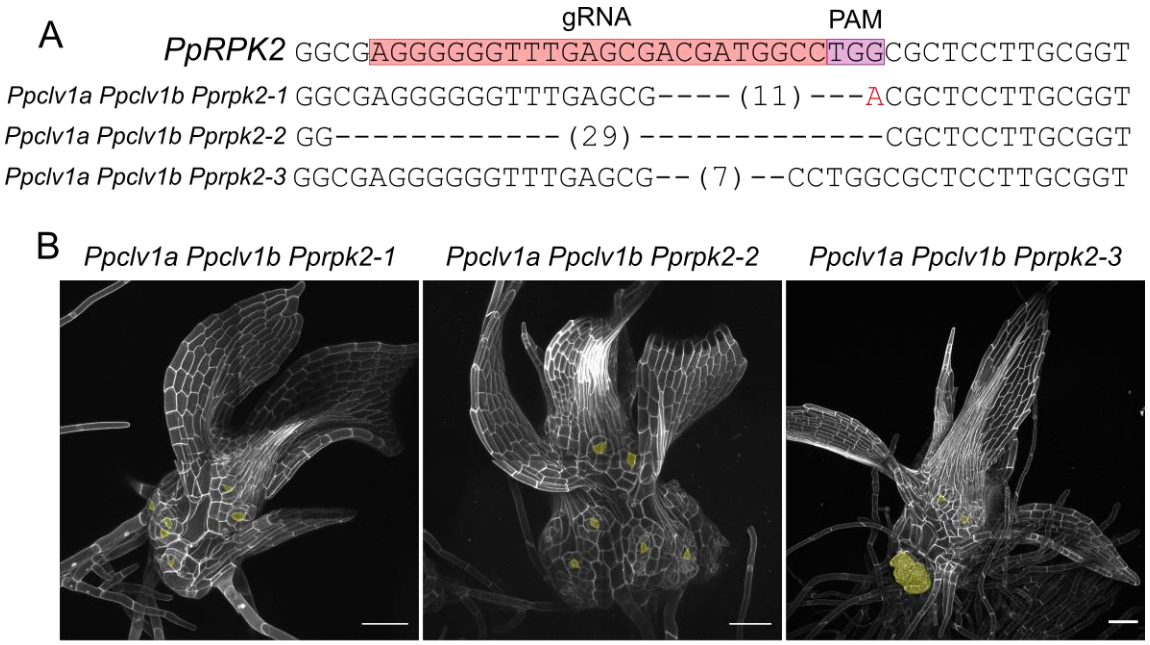

Supplemental Figure 1: Characterization of three *Ppclv1a Ppclv1b Pprpk2* triple mutant lines. We transformed *Ppclv1a Ppclv1b-8* double mutants (Whitewoods, Cammarata et al. 2018) with plasmids expressing a *PpRPK2*-targeting gRNA, Cas9, and a selectable marker. We generated independent lines with *Pprpk2*-like colony phenotypes and selected three for in-depth phenotyping of gametophore morphogenesis, shown here. **A)** Portion of *PpRPK2* exon 1 with gRNA target sequence and PAM (Protospacer Adjacent Motif) highlighted. Below, aligned sequences of the *Pprpk2* mutant loci from three *Ppclv1 Pprpk2* lines. **B)** All *Ppclv1 Pprpk2* mutants display the short stature, ectopic stem cell phenotypes, and ectopic midrib specification representative of a combination of *Ppclv1* and *Pprpk2* phenotypes.

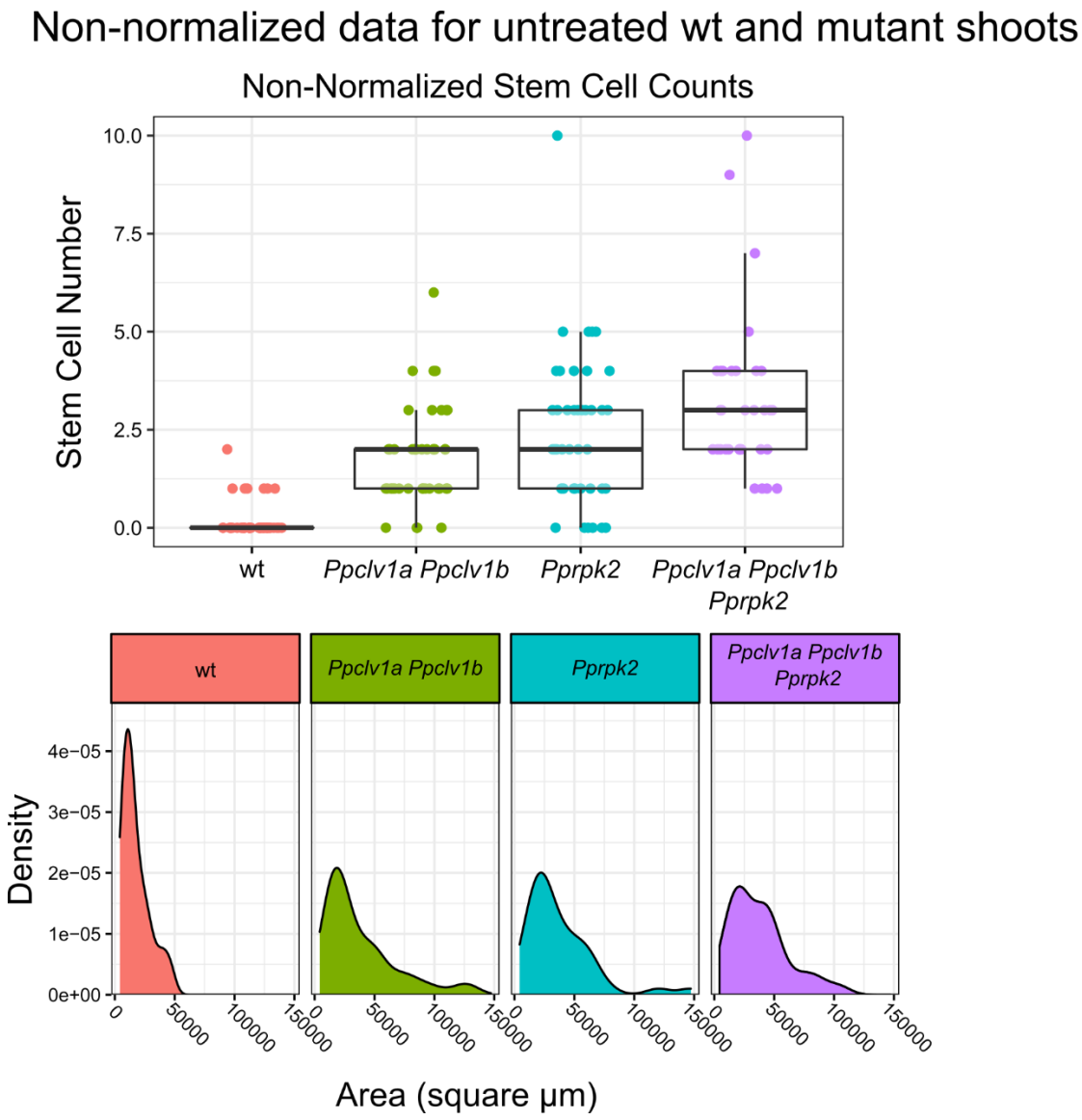

Supplemental Figure 2: Non-normalized data set of wt, *Ppclv1a Ppclv1b*, *Pprpk2*, and *Ppclv1a Ppclv1b Pprpk2* gametophores. Top panel: boxplot representing raw number of stem cells observed on gametophores at each condition. Lower panel: density plot showing distribution of stem areas from which stem cell measurements were taken.

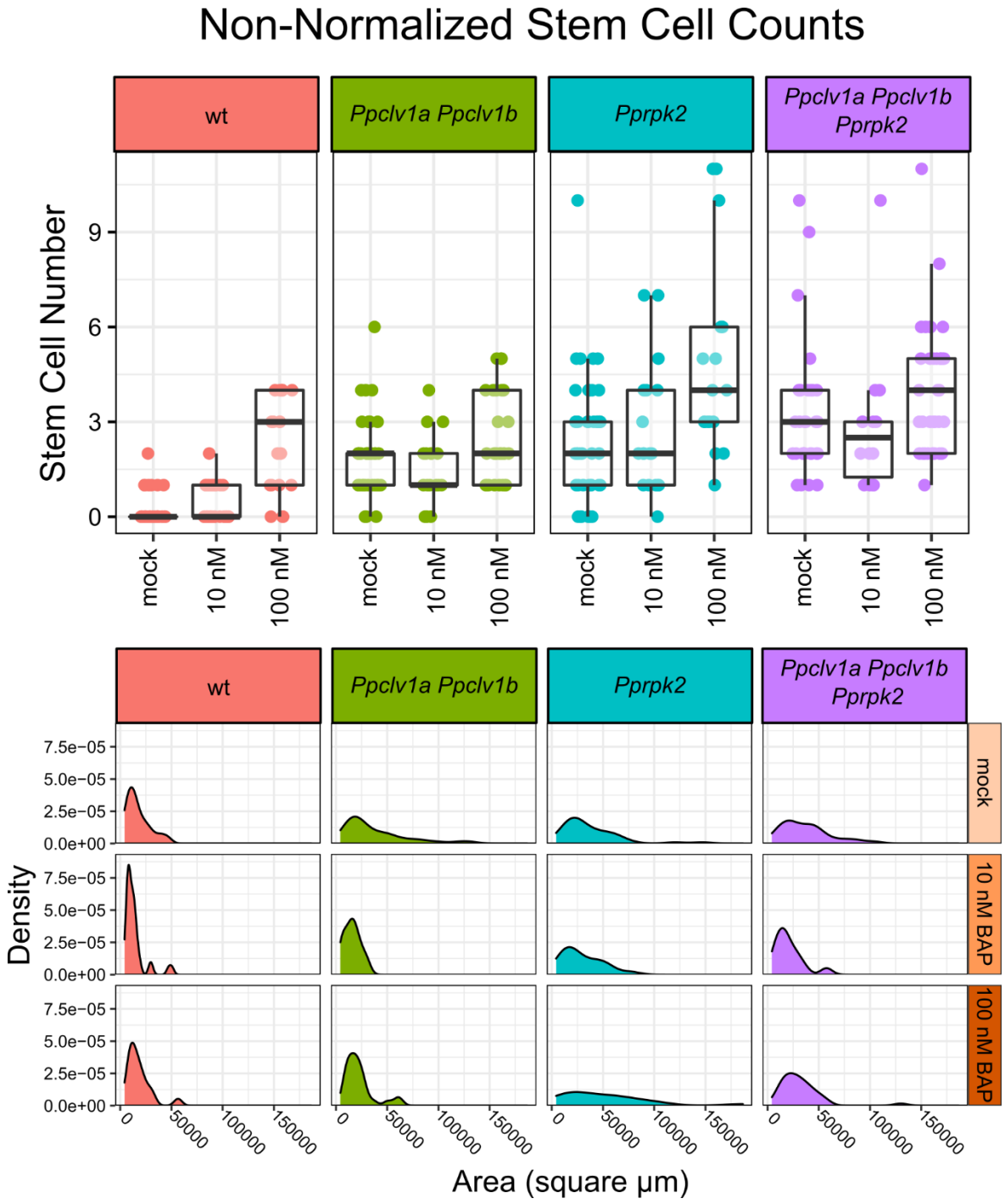

Supplemental Figure 3: Non-normalized data set of mock and cytokinin-treated wt, *Ppclv1a Ppclv1b*, *Pprpk2*, and *Ppclv1a Ppclv1b Pprpk2* gametophores. Top panel: boxplot representing raw number of stem cells observed on gametophores at each condition. The normalized data is presented in Figure 3M. Lower panel: density plot showing distribution of stem areas from which stem cell measurements were taken. Includes data from Supplemental Figure 2 to parallel main text. See results section for statistics from Poisson regression.

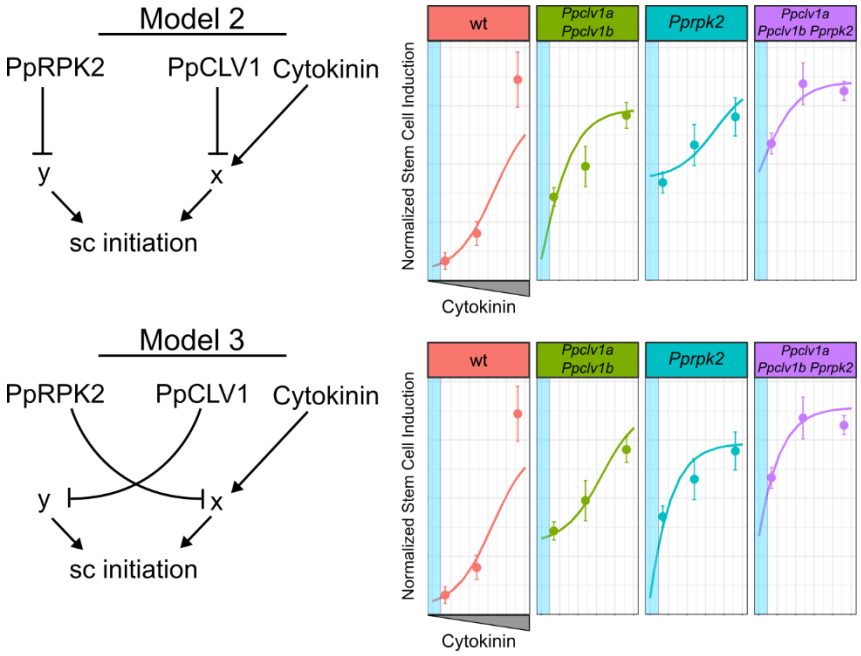

Supplemental Figure 4: Predictions of stem cell initiation at zero cytokinin. The best performing models of stem cell initiation in wild type *Ppclv1a Ppclv1b*, *Pprpk2*, and *Ppclv1a Ppclv1b Pprpk2* triple mutants with and without exogenous cytokinin were used to predict stem cell initiation levels if cytokinin signaling were abolished (highlighted blue). Each model predicted a reduction in stem cell initiation. More informatively, mutants of whichever gene that acts upstream of *x* would see their stem cell initiation phenotypes fully suppressed upon reduced cytokinin (*PpRPK2* above, *PpCLV1* below). Data points and error bars represent empirical stem cell per area values normalized to wild type grown on mock-treated media. From left to right: mock, 10 nM BAP, 100 nM BAP. Solid lines represent model simulations after optimization of parameters to the data.

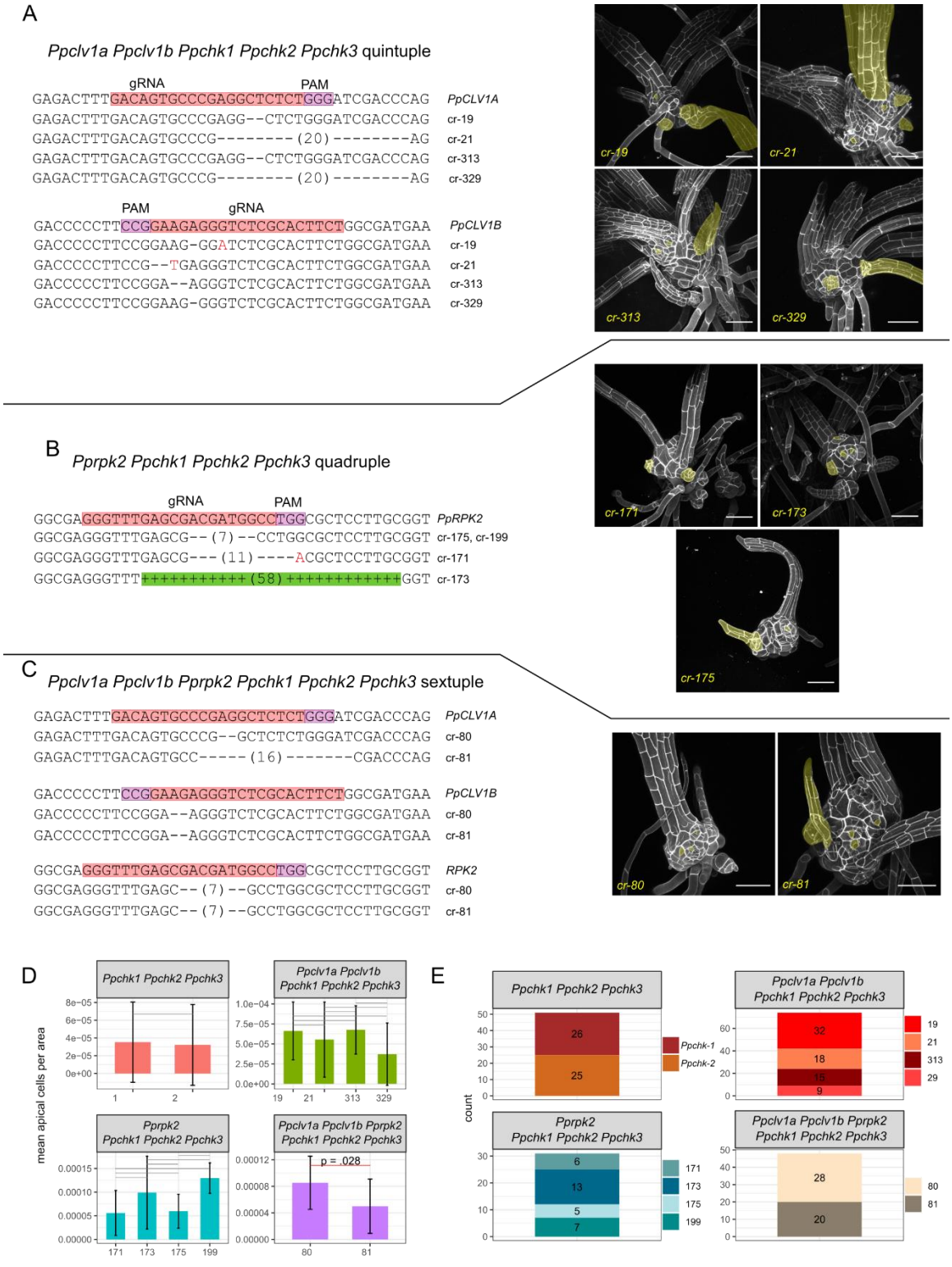

Supplemental Figure 5: genotyping higher order *Ppclv1 Pprpk2 Ppchk* mutants. *Ppchk1 Ppchk2 Ppchk3-1* plants were transformed with gRNAs targeting *PpCLV1a* and *PpCLV1b*, *PpRPK2*, or all three. Three independent lines for *Ppclv1a Ppclv1b Ppchk1 Ppchk2 Ppchk3* quintuple mutants (A) and *Pprpk2 Ppchk1 Ppchk2 Ppchk3* quadruple mutants were obtained (B). A *Ppclv1b Pprpk2 Ppchk1 Ppchk2*

Ppchk3 quintuple mutant line was recovered and re-transformed with a *PpCLV1α*-targeting gRNA to generate two sextuple mutant lines (C). CRISPR mutant lines are indicated with *cr-#*. On the right, examples of gametophore phenotypes for each of these lines show a combination of *Ppclv1, Pprpk2*, and *Ppchk* phenotypes. Comparison of stem cell phenotype across mutant lines, with pairwise tests showing that no lines are significantly different from any other of the same genotype except for *cr-80* and *cr-81* (D). Non-significant results (Bonferroni correction-adjusted $p > 0.05$) are represented by gray lines; significant results in red. Distribution of lines used to generate the data for each genotype (E).

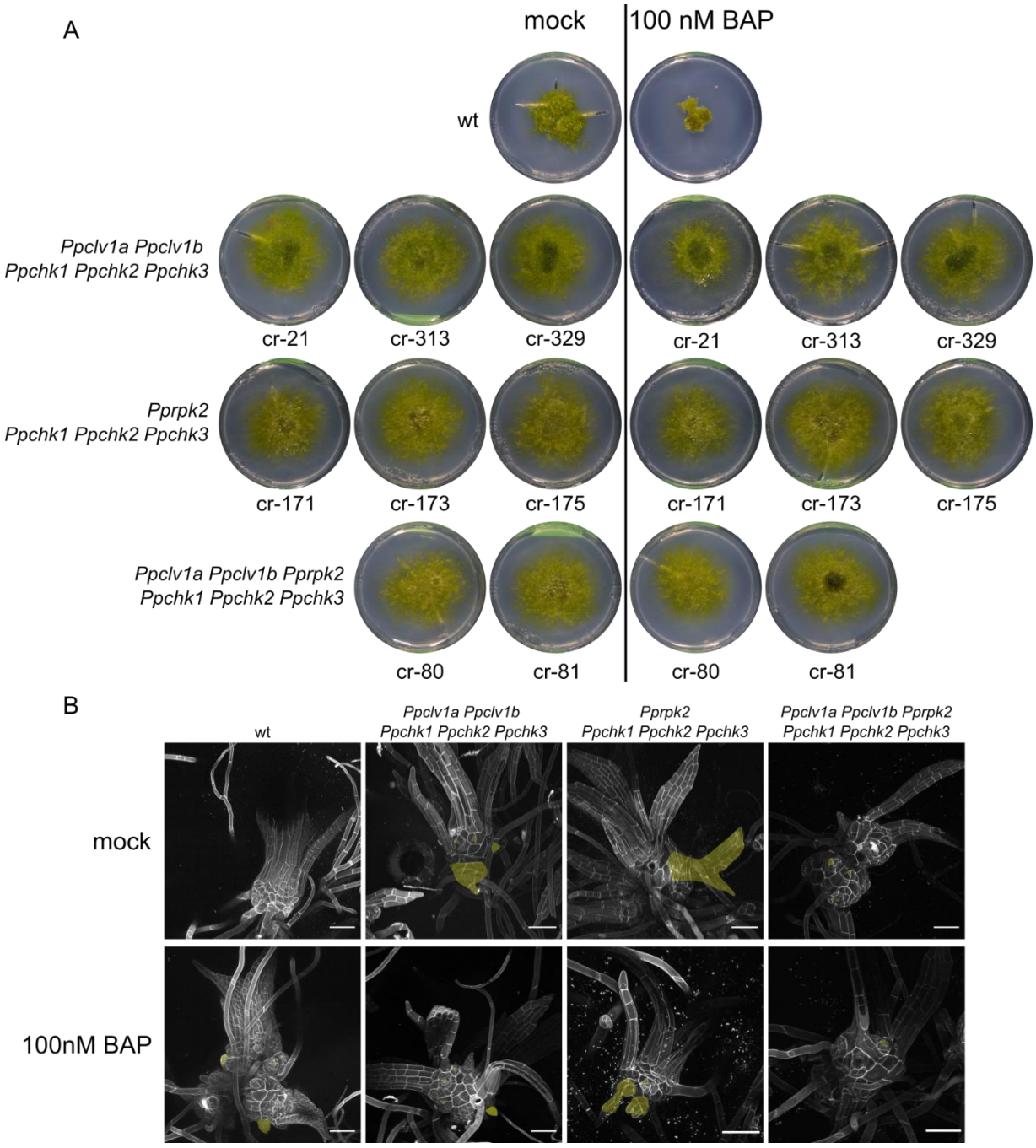

Supplemental Figure 6: *Ppchk* mutants are insensitive to cytokinin. A) Five week-old *P. patens* tufts grown on mock (left) or 100 nM BAP (right). From top to bottom, wild type, *Ppclv1a Ppclv1b Ppchk1 Ppchk2 Ppchk3*, *Pprpk2 Ppchk1 Ppchk2 Ppchk3*, and *Ppclv1a Ppclv1b Pprpk2 Ppchk1 Ppchk2 Ppchk3* mutants with independent mutant lines tested. B) Confocal images of gametophores from colonies in panel A. Wild type *P. patens* responds to 100 nM BAP whereas *Ppchk1 Ppchk2 Ppchk3* mutant lines do not.

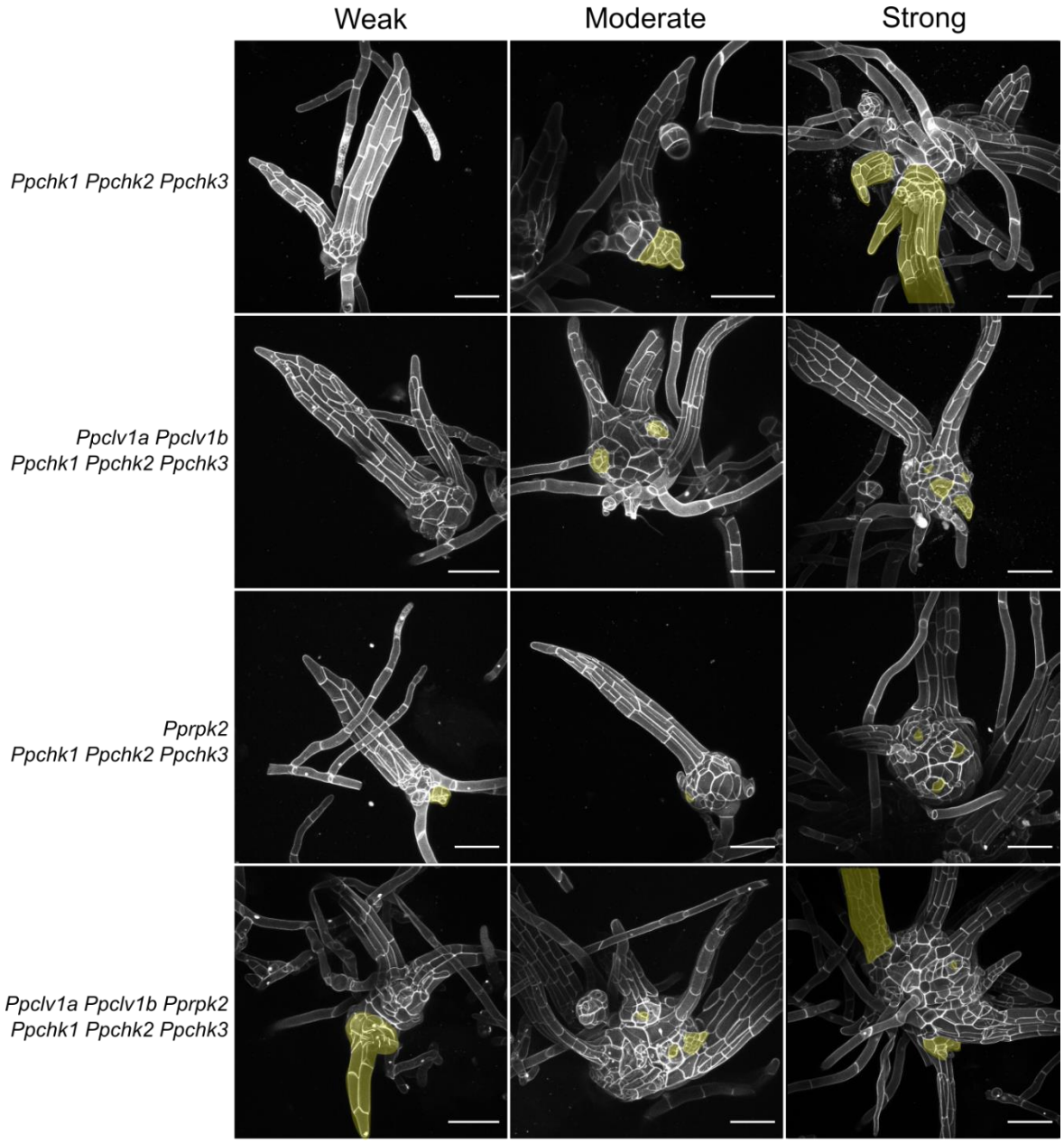

Supplemental Figure 7: Higher order *Ppclv1, Pprpk2,* and *Ppchk* mutant phenotypes are variable. Examples of weak, moderate, and strong phenotypes observed for *Ppchk* mutant gametophores and each higher order *Ppclv1 Ppchk, Pprpk2 Ppchk*, and *Ppclv1 Pprpk2 Ppchk* mutants. *Pprpk2 Ppchk1 Ppchk2 Ppchk3* quadruple mutant phenotypes were particularly variable. However, when quantified these lines still presented an increased initiation of stem cells per area (Figure 5 E).

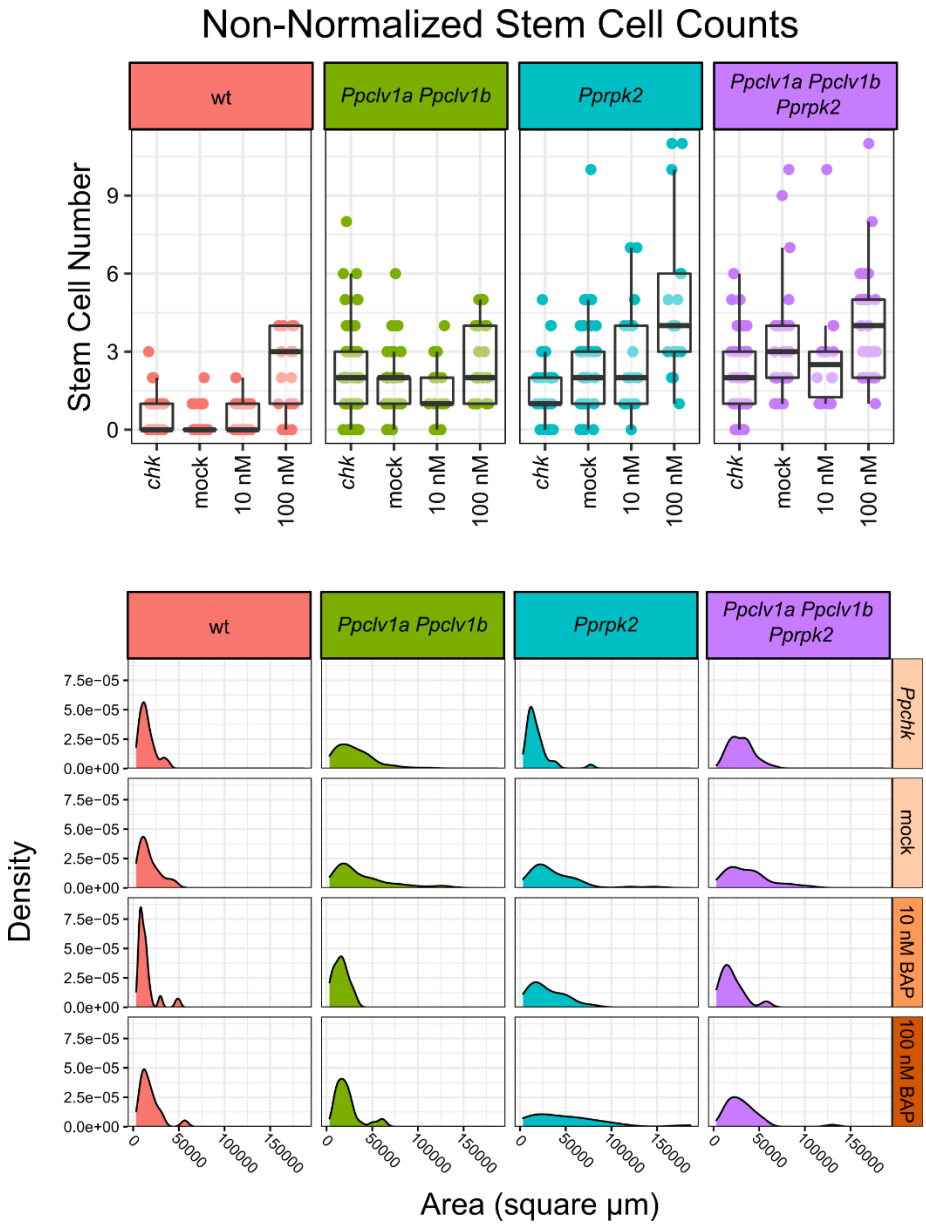

Supplemental Figure 8: Full non-normalized data set. Top panel: boxplot representing raw number of stem cells observed on gametophores at each condition. The normalized data is presented in Figure 5E. Lower panel: density plot showing distribution of stem areas from which stem cell measurements were taken. Here are the data for all gametophores measured across genotypes and treatment conditions. Includes data from supplemental figure 3 to parallel main text. See results section for statistics from Poisson regression.

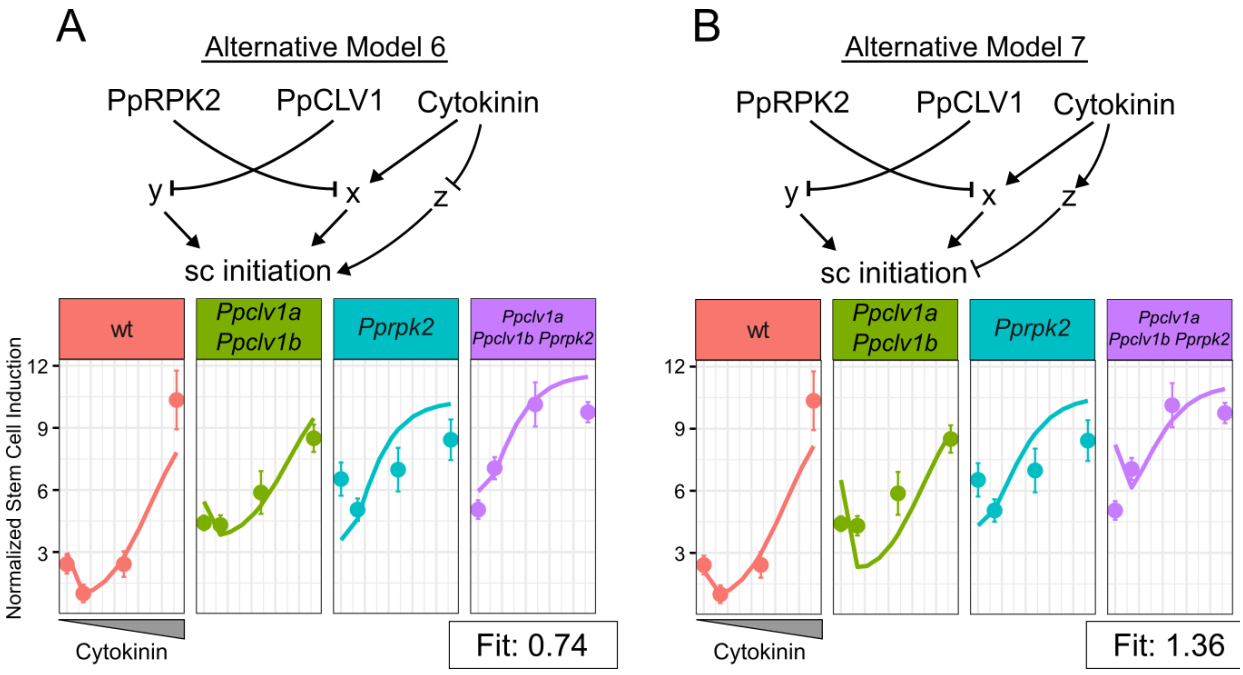

Supplemental Figure 9: Models fit poorly with *PpRPK2* upstream of cytokinin response. Alternative versions of models 6 and 7 (Figure 5), with *PpRPK2* upstream of cytokinin-mediated stem cell induction (x). To Solid lines represent simulated data while dots represent mean stem cells per area from the empirical data. Error bars show the standard error. The x axis shows a log transformation of the cytokinin value input to the model.

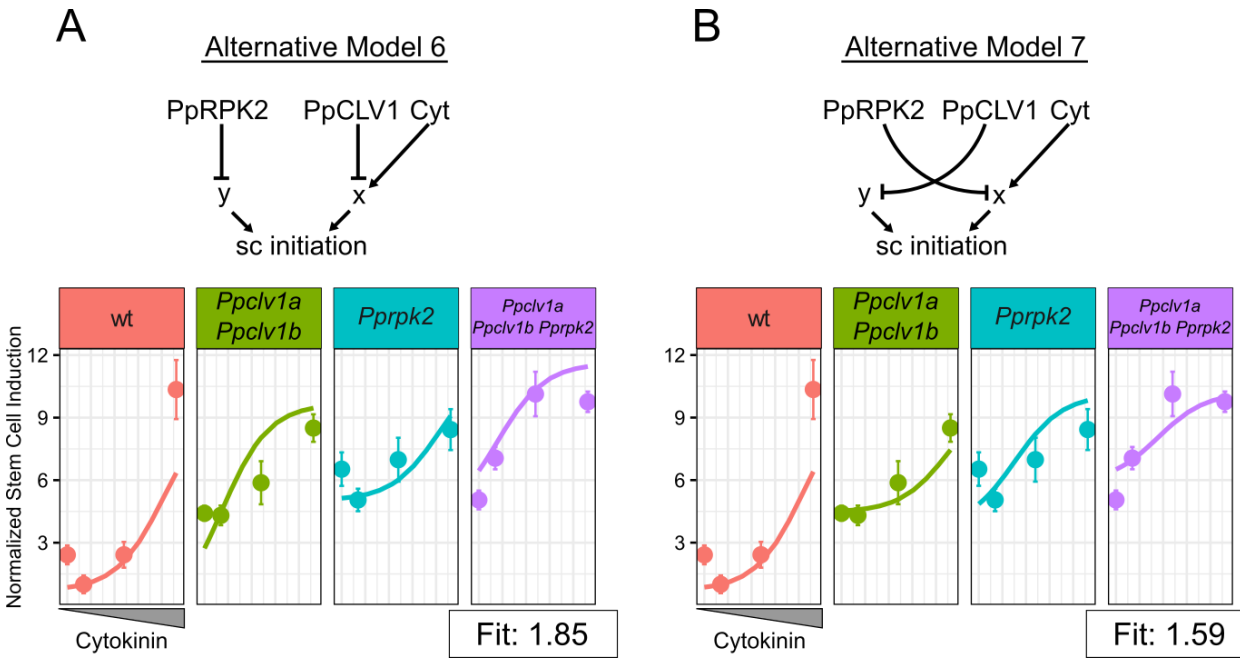

Supplemental Figure 10: Models lacking incoherent feed-forward control cannot recapitulate *Ppchk* and higher order *Ppclv Pprpk2 Ppchk* phenotypes. The models that best fit the stem cell phenotypes of wt, *Ppclv1a Ppclv1b*, *Pprpk2*, and *Ppclv1a Ppclv1b Pprpk2* gametophores on mock and cytokinin treatments were fit to the full dataset including the *Ppchk1 Ppchk2 Ppchk3* and higher order *Ppclv1, Pprpk2, Ppchk* mutants (leftmost datapoint on each plot). Dots represent empirical data; lines represent simulated data.

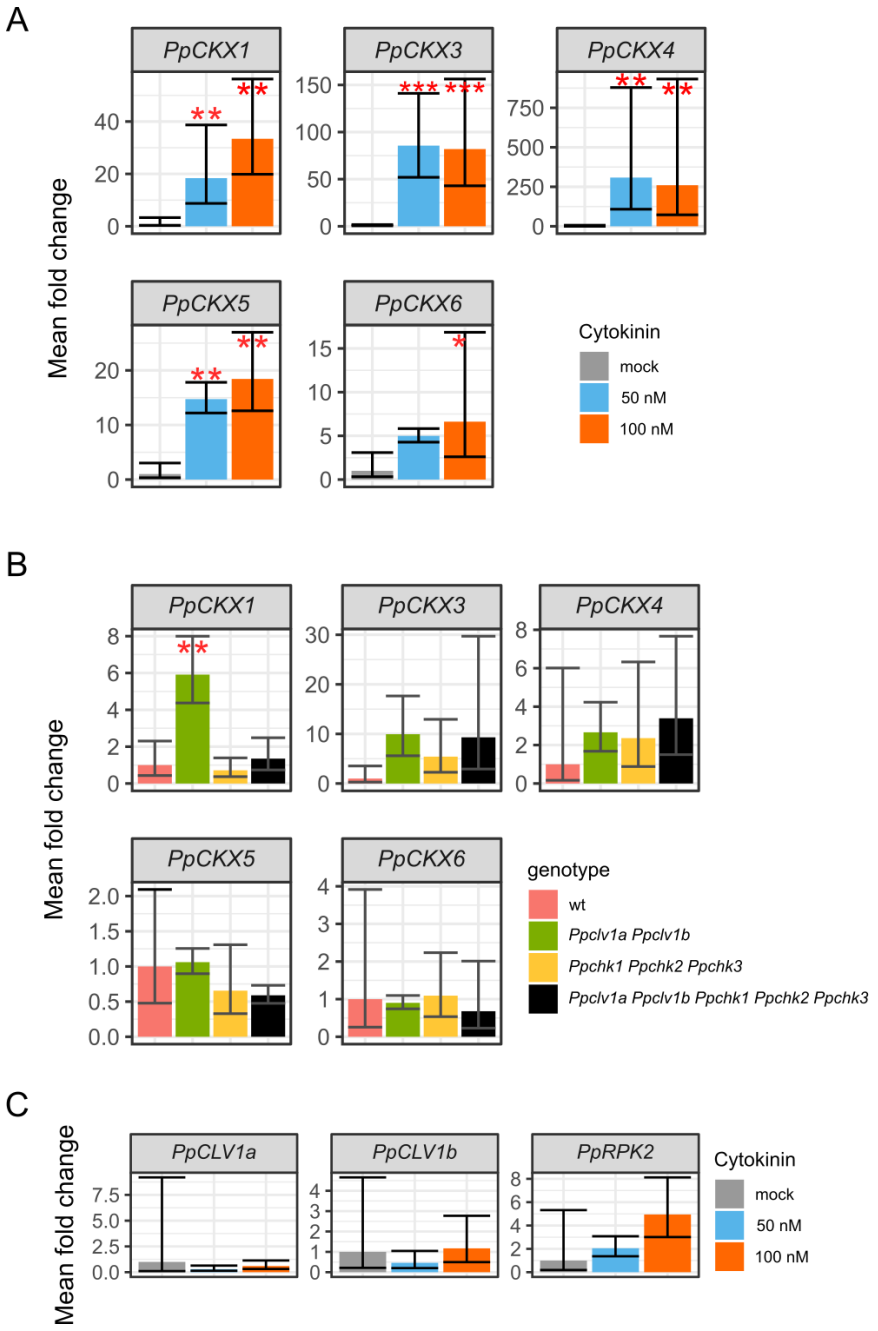

Supplemental Figure 11: Gene expression analysis testing cytokinin, *Pp*CLV1, and *Pp*RPK2 interactions. A) qPCR-data testing the change in expression of five *PpCKX* genes in response to growth on cytokinin. All *PpCKX* genes tested were upregulated, although *PpCKX6* weekly so. B) *PpCKX* gene expression was used as an indicator of cytokinin transcriptional response. *PpCKX1* expression was increased in *Ppclv1a Ppclv1b,* but unchanged in *Ppclv1a Ppclv1b Ppchk1 Ppchk2 Ppchk3*, supporting a role for *PpCLV1* in inhibiting cytokinin response. However, other *PpCKX genes* tested did not display this same trend. C) Expression levels of *PpCLV1a, PpCLV1b*, and *PpRPK2* were unchanged due to growth on cytokinin.

Supplemental Table 1 primers

oJCm278	GAGTTAGGGGAGATGACGCG	*PpRPK2* gRNA target locus genotyping
oJCm279	CTTGGAGGACTCACCAACCC	*PpRPK2* gRNA target locus genotyping
oJCm379	cacctaaacggctcaattcc	*PpCLV1a* exon 4 genotyping
oJCm380	tgatgatctccgatggtatgg	*PpCLV1a* exon 4 genotyping
oJCm181	tggagagacgcaacttccat	*PpCLV1b* exon 1 sample – sgRNAs 1 and 2
oJCm182	ttaagacgccccaaatcagc	*PpCLV1b* exon1 sample – sgRNAs 1 and 2
oJCm175	gcttcGAGCTCGAATTCAGA	PpU3 promoter forward for Sanger sequencing of gRNA plasmids
oJCm176	ggtcGACGAGCTCAAAAAAAG	sgRNA_scaffold_reverse for Sanger sequencing of gRNA plasmids
oJCm208	GAGCTCGAATTCGTCCATTGA	PpU6 promoter forward for Sanger sequencing of gRNA plasmids
oJCm375	ACGGACATTGCATTTAAGACCT	qRT Primer REF gene F: 60s
oJCm376	GTCGATTACCTGTGGAGAAGAC	qRT Primer REF gene R: 60s
oJCm360	ATTTGTGGATGCTGCTGGTG	*PpCKX5* qRT-PCR primer F
oJCm361	ACGTTGCTAATTTCAGGTCCG	*PpCKX5* qRT-PCR primer R
oJCm362	CGAAAGTACCTGGAGTCGCT	*PpCKX1* qRT-PCR primer F
oJCm363	CAGACTCTAACCTCGCCACA	*PpCKX1* qRT-PCR primer R
oJCm364	AATTCACGAGCTGGGTTCAC	*PpCKX4* qRT-PCR primer F
oJCm365	AGAGCGACTCCAGGTACATG	*PpCKX4* qRT-PCR primer R
oJCm366	TAGACGTCCTGAAAGCCTCT	*PpCKX6* qRT-PCR primer F
oJCm367	ACGACTTCCAGCTGCAGAA	*PpCKX6* qRT-PCR primer R
oJCm368	CTGGTCTAGAGCCCTTCACC	*PpCKX3* qRT-PCR primer F
oJCm369	CCAGCTTTGTCCAGATTCCG	*PpCKX3* qRT-PCR primer R
oJCm383	GTATTGGTCCTGAGAGTGG	*PpCLV1a* qRT-PCR primer F
oJCm384	GAGGTTCACACACACACAAG	*PpCLV1a* qRT-PCR primer R
oJCm387	TTTCAAGACACTGGCAAATC	*PpCLV1b* qRT-PCR primer F
oJCm388	TGCTTCAATCGGTCTCTTAC	*PpCLV1b* qRT-PCR primer R
oJCm391	CACCAGCACCAACATAAAC	*PpRPK2* qRT-PCR primer F
oJCm392	TACAGCAACCACCAATCC	*PpRPK2* qRT-PCR primer R

Supplemental Table 2 gRNA oligonucleotides

sgRNA Oligo for synthesis	**Sequence**	**Target**	**Inserted into Vector**
sgJTC5	GGCAgacagtgcccgaggctctct	*PpCLV1a* exon4 cds	U3_BSAI-sgRNA
sgJTC6	AAACagagagcctcgggcactgtc	*PpCLV1a* exon4 cds*	U3_BSAI-sgRNA

sgJTC9	GGCagaagtgcgagaccctcttc	*PpCLV1b* exon1 cds sgRNA1	U3_BSAI-sgRNA
sgJTC10	AAACgaagagggtctcgcacttc	*PpCLV1b* exon1 cds sgRNA1*	U3_BSAI-sgRNA
sgJTC105	catGGGTTTGAGCGACGATGGCC	*PpRPK2* cds	U6_sgRNA
sgJTC106	aaacGGCCATCGTCGCTCAAACCC	*PpRPK2* cds	U6_sgRNA

Supplemental Table 3: Genes referenced in this study

Full Gene Name	**Alias**	**Version 1.6**	**Version 3**
PpCLAVATA1a	*PpCLV1a*	Pp1s14_447V6	Pp3c6_21940
PpCLAVATA1b	*PpCLV1B*	Pp1s5_68V6	Pp3c13_13360
PpRECEPTOR-LIKE PROTEIN KINASE 2	*PpRPK2*	Pp1s311_57V6	Pp3c7_5570
PpCYTOKININ HISTIDINE KINASE 1	*PpCHK1*	Pp1s50_141V6	Pp3c25_8540
PpCYTOKININ HISTIDINE KINASE 2	*PpCHK2*	Pp1s194_72V6	Pp3c16_7610
PpCYTOKININ HISTIDINE KINASE 3	*PpCHK3*	Pp1s252_49V6	Pp3c6_7030
PpCYTOKININ OXIDASES 1	*PpCKX1*	Pp1s152_115V6	Pp3c20_2380V3
PpCYTOKININ OXIDASES 3	*PpCKX3*	Pp1s222_49V6	Pp3c23_17550V3
PpCYTOKININ OXIDASES 4	*PpCKX4*	Pp1s222_68V6	Pp3c23_17360V3
PpCYTOKININ OXIDASES 5	*PpCKX5*	Pp1s403_31V6	Pp3c24_13960V3
PpCYTOKININ OXIDASES 6	*PpCKX6*	Pp1s595_6V6	Pp3c8_18580V3
60S RIBOSOMAL PROTEIN	60s	Pp1s79_255V6	Pp3c14_7550V3

Supplemental Table 4: Media and Solutions

Media		
Stock Solutions for BCD and BCDAT moss growth media		
Stock solution B (100x)	$MgSO_4 \cdot 7H_2O$ **or** $MgSO_4$ (anhydrous)	2.5 g 1.2 g
	dH_2O	Fill to 100 ml
Stock solution C (100x)	KH_2PO_4	2.5 g
	dH_2O	Fill to 50 ml
	Adjust pH with 4 M KOH	
	dH_2O	Fill to 100 ml
Stock Solution D (100x)	KNO_3	10.1 g
	$FeSO_4 \cdot 7H_2O$	0.125 g
	dH_2O	Fill to 100 ml

Ammonium tartrate (100x)	di-ammonium (+) tartrate	9.2 g
	dH_2O	Fill to 100ml
Trace element solution (20,000x)	H_3BO_3	614 mg
	$AlK(SO_4)_2 \cdot 12\ H_2O$	55 mg
	$CuSO_4 \cdot_5\ H_2O$	55 mg
	KBr	28 mg
	LiCl	28 mg
	$MnCl_2 \cdot 4\ H_2O$	389 mg
	$CoCl_2 \cdot 6\ H_2O$	55 mg
	$ZnSO_4 \cdot 7\ H_2O$	55 mg
	KI	28 mg
	$SnCl_2 \cdot 2\ H_2O$	28 mg
	dH_2O	Fill to 50 ml
$CaCl_2$ (500x) Add after autoclaving	$CaCl_2$	3.67 g
	dH_2O	Fill to 50 ml
Solutions for transformation		
8.5% Mannitol	Mannitol	85 g
	dH_2O	1 L
Driselase	Driselase	4 g
	8.5% Mannitol	200 ml
	Gently stir for 30 minutes at room temperature. Keep at 4°C for 30 minutes. Stir 5 minutes at room temperature. Spin at 2,500g for 10 minutes in 50 ml Falcon Tubes. Filter sterilize with 0.22 µm filter. Aliquot 10 ml into 15 ml Falcon Tubes.	
3M Solution	Mannitol	4.5g
	1M $MgCl_2 \cdot 6H_2O$	750 µl
	1% MES pH 5.6	5 ml
	H_2O	to 50 ml
PEG Solution for Transformation	8.5% Mannitol	9 ml
	1M $Ca(NO_3)_2 \cdot 4H_2O$	1 ml
	1M Tris pH 8.0	100 µl
	PEG 8000	4 g, melted slowly in microwave
PRMB	BCDAT	
	Mannitol	6% (w/v)
	Agar	0.55% (w/v)
	500 mM $CaCl_2$ (add after autoclaving)	1 ml per 50 ml media
PRMT	BCDAT	
	Mannitol	6% (w/v)
	Agar	0.3% (w/v)

	500 mM $CaCl_2$ (add after melting)	1 ml per 50 ml media

Dynamical Model Methods

Systems of ordinary differential equations can be used to simulate how values of interacting variables change over time. In the case of a genetic or developmental network these variables can represent gene expression levels or the strength of signaling pathway outputs. We used such dynamical models to assess how well competing hypothetical stem cell regulatory network topologies could reconstitute the data. Each of the models described here simulated the accumulation of gene products through time, simultaneously modeling transcription and translation. The equations are modified from Gordon et al. 2009, where the authors use similar systems of differential equations to test predictions about CLV3, CLV1, WUS, and cytokinin interactions in Arabidopsis(Gordon et al., 2009).

Model 1-5

Models 1-5 consist of the following equations. Edges in the network (such as RPK2 inhibition of y) were changed by setting corresponding *k* values (in the case of RPK2 and y, *k*[5] to 0).

$$\frac{dx}{dt} = \frac{p_1 + cyt * k_1}{1 + p_1 + cyt * k_1 + k_2 * clv + k_3 * rpk2} - d_1 * x$$

$$\frac{dy}{dt} = \frac{p_2}{1 + p_2 + k_4 * clv + k_5 * rpk2} - y * d_2$$

$$\frac{dinit}{dt} = \frac{p_3 + x * k_6 + y * k_7}{1 + p_3 + x * k_6 + y * k_7} - init * d_3$$

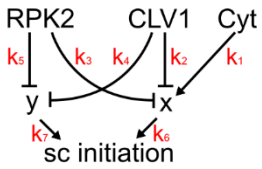

Model 6 and 7

Models 6 and 7 are similar in topology with the inclusion of the variable *z* downstream of cytokinin. In Model 6, *z* is inhibited by cytokinin, and induces *init*. In model 7, *z* is induced by cytokinin, and inhibits *init*. Two versions of each model were run: one with CLV1 inhibiting *x* and RPK2 inhibiting *y*, and one RPK2 inhibits *x* and CLV1 inhibits *y*.

Model 6

$$\frac{dx}{dt} = \frac{p_1 + cyt * k_1}{1 + p_1 + cyt * k_1 + clv * k_2 + rpk2 * k_3 + z * k_9} - x * d_1$$

$$\frac{\mathrm{dy}}{\mathrm{dt}} = \frac{p_2}{1 + p_2 + clv * k_4 + rpk2 * k_5} - \mathrm{y} * \mathrm{d}_2$$

$$\frac{dz}{dt} = \frac{p_4}{1 + p_4 + cyt * k_8} - z * d_4$$

$$\frac{dinit}{dt} = \frac{p_3 + x * k_6 + y * k_7 + z * k_9}{1 + p_3 + x * k_6 + y * k_7 + z * k_9} - init * d_3$$

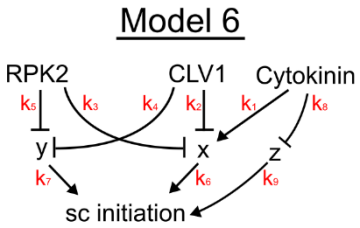

Model 7

$$\frac{dx}{dt} = \frac{p_1 + cyt * k_1}{1 + p_1 + cyt * k_1 + clv * k_2 + rpk2 * k_3 + z * k_9} - x * d_1$$

$$\frac{dz}{dt} = \frac{p_4 + cyt * k_8 * cyt}{1 + p_4 + cyt * k_8} - z * d_4$$

$$\frac{dy}{dt} = \frac{p_2}{1 + p_2 + clv * k_4 + rpk2 * k_5} - y * d_2$$

$$\frac{dinit}{dt} = \frac{p_3 + x * k_6 + y * k_7}{1 + p_3 + x * k_6 + y * k_7 + z * k_9} - init * d_3$$

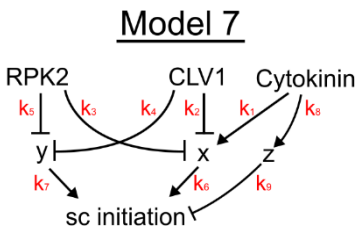

Model Variables

The variables used in this work are summarized here:

Variable	Describes
x	Cytokinin-response pathway that induces stem cell formation
y	Cytokinin-independent pathway inducing stem cell formation
z	Cytokinin feedforward control of stem cell formation
init	Level of stem cell initiation
clv	Strength of CLV1 signaling. This is a static, non-dynamical parameter
rpk2	Strength of RPK2 signaling. This is a static, non-dynamical parameter
cyt	Strength of cytokinin signaling. Set to 0 for *chk*, 1 for mock-treated wt, and to 10 and 100 for cytokinin treatments

It is important to note that these variables are not meant to exactly reflect the level of a protein, but more the presence/absence and strength of the signaling pathway.

Model parameters

Each equation in the model describes how one of the above variables changes over time. The change over time is proportional to the current value of the parameters and other variables in the model. Each of the other variables in an equation is associated with a proportionality constant that describes how that variable affects the accumulation rate described by that equation. Additionally, a differential equation might include a term to describe accumulation independent of the other variables as well as degradation rates. These constants were assigned to the following categories:

- p = production; describes basal accumulation rates
- d = degradation; describes degradation rates
- k = interaction coefficient/proportionality constant

Each model also used a set of initial conditions (a vector called *base*)and a time vector that ran the model over 2000 or 3000 time intervals.

Summary of workflow

1) Run the model and confirm that it converges to a steady-state value within the allotted steps.
2) Simulate each mutant genotype at each cytokinin level of interest with the initial parameters to generate a starting fit score.
3) Optimize parameters and determine fit to empirical data

1) Running a model

Each model was solved using the LSODA solver for Ordinary Differential Equations (ODEs) and the R statistical programming language Version 4.0.2(Soetaert et al., 2010; Team, 2016). Models were

confirmed to converge to steady state values before and after each run of the optimizer, as determined by each variable reaching a plateau by the end of the modeled time period. All plotting used the ggplot2 package(Hadley et al., 2016). Models were run for 2000 or 3000 time points (steps) distributed over 200 or 300 'seconds', as depicted by the sample model run below. Dynamical variables change through time and converge at steady state values. The final values at time 200 or 300 (more steps were given to models that took longer to converge) were taken and stored as the output of the model.

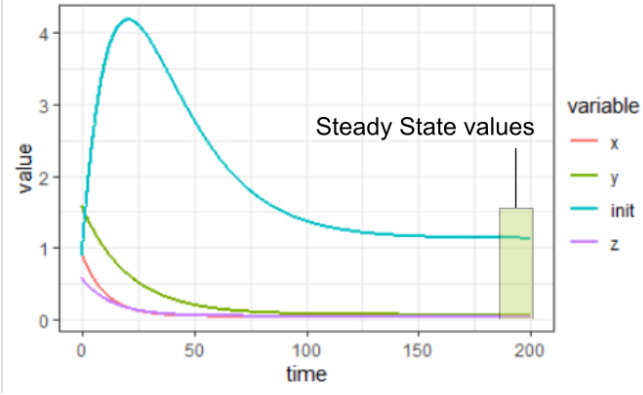

2) Simulate mutant genotypes and different levels of cytokinin

To simulate mutant genotypes in models 1-7, we set CLV1 or RPK2 to 0 and their synthesis parameters to 0. Cytokinin was coded as a static parameter and altered in the following ways to simulate different conditions from our experimental datasets:

Cytokinin value	Simulates the condition
0	*chk* triple mutant
1*	growth on minimal media (BCD) with wild type *CHK* genes
10	10 nM BAP
100	100 nM BAP

* As '1' here is somewhat arbitrary, we also tried values of 0.5 and 0.75 in its stead, which did not significantly change the model outputs (not shown).

3) Optimization of the fit to the empirical data

We used an optimizer to identify the parameter values of *k, p*, *d*, and *base* for which the model output best fit the empirical data. Each model was initially run with semi-arbitrary parameters that allowed the model to converge within the given time frame. We started each model from a similar starting parameter set before optimization.

To optimize the model parameters, we first needed to be able to compare the model output with the empirical data. Comparing the simulated data to the empirical data required that the two datasets be normalized to a unified scale. To achieve this, the empirical data set was normalized to the ectopic stem cell per area value of wild type moss grown on minimal media. For the model, 'area' was not considered, and the modeled stem cell initiation values (termed init) were also normalized to the modeled stem cell values of wild type on minimal media (cytokinin = 1). This allowed us to compare the trends in the data, for instance if *clv1* mutants on minimal media made four times as many stem cells per area as wild type on minimal media, we assigned a value of four to this condition in the dataset. The model optimizer would then attempt to converge on parameters that yielded stem cell initiation values for *clv1* mutants

at the minimal media cytokinin input parameter that was four times higher than wild type at the same cytokinin level. After normalization, each simulated value was compared to its corresponding empirical data value to generate a fit score (F). These scores were used to penalize a model with a given set of parameters; higher scores were worse than lower scores. The score was intended to accomplish the following:

1) Equally penalize simulated values that overshot or undershot the data
2) Weigh all datapoints equally, regardless of magnitude. To do this, the score had to **minimize fold changes between the simulated and empirical data**. Otherwise, a change from 1->2 would be penalized less than a change from 10 to 14, despite the former constituting a much larger relative change.
3) Penalize larger deviations from the data more severely than smaller ones. Otherwise, a model might be 'optimized' to have good fits to some data points but terrible fits to others. Since the intention of the model is to capture the trends in the data across all conditions, such a scenario was unacceptable.

We used the log of the fold change between the simulated (m_i) and empirical data (d_i) to accomplish the above aims one and two, and then squared to accomplish aim 3. The sum of these penalty scores at each data point (P_i) then yielded the total fit score *F*:

$$P_i = \ln\left(\frac{m_i}{d_i}\right)$$

$$F = \sum {P_i}^2$$

After each run, new model parameters *k, p*, *d*, and *base* were randomly selected from a normal distribution based around the previous parameter value and the model was run again. The standard deviation of the distribution was 0.1. The Fit Score *F* for the new model was compared with the previous *F*. If the new *F* proved lower than the previous, then the new model parameters were saved and mutated (used as the mean of the normal distribution from which the next parameter value was selected) again for the next run. If instead the new *F* was not lower than the previous, the original parameter set was randomly mutated again. The optimizer was run for 200-300 iterations, after which the fit scores no longer meaningfully changed. We then compared the best fit scores generated by each model after optimization to determine which network architecture(s) were most likely given their ability to reproduce the data.

On Poisson coefficients

Poisson coefficients are akin to Beta values reported by linear regressions, in that they are proportional to the expected change in the dependent variable given the change in independent variable associated with the coefficient. In the case of a Poisson coefficient, the exponentiation of the coefficient tells you the predicted effect due to the change in factor level. For instance, with a Poisson coefficient of 0.64, the estimated change in apical cell number due to the *clv1* mutation is ~1.9 (= e^0.64). It is important to note that our models make use of both categorical and continuous variables, which makes the coefficients appear deceptively different in magnitude. For example, the coefficient associated with exogenous cytokinin is small because cytokinin is coded as a continuous variable. The coefficient is 0.013 and it's exponent is 1.013, which appears much lower than the expected change due to *clv1* of 1.9. However, the cytokinin coefficient of 1.013 shows the predicted change per unit cytokinin. The predicted change for 10nM BAP is the exponentiation of 10*the coefficient, so e^(10*.013) = 1.14.

Going on to predict the change for 100nM bap is e^(1.3) = 3.67. Finally, these numbers represent the fold change from the 'intercept' value also reported by the model.

List of parameters, starting values, and finishing values for a sample run

Model 1 (Figure 4 A)

Parameter	Description	Starting Value	Finishing Value
k_1	cytokinin ↑ x	1	1.500644
k_2	clv ↓ x	1	0.525365
k_3	rpk2 ↓ x	1	20.8025
k_4	clv ↓ y	1	4.652118
k_5	rpk2 ↓ y	1	0.190285
k_6	x ↑ init	0.1	0.019766
k_7	y ↑ init	0.1	0.319337
p_1	basal x synthesis	.01	0.00365
p_2	basal y synthesis	0.01	0.02994
p_3	basal init synthesis	0.01	0.008979
d_1	x degradation	0.05	0.035265
d_2	y degradation	0.05	0.035136
d_3	init degradation	0.05	0.02294
$base_1$	initial x	1	1.165125
$base_2$	initial y	1	0.84229
$base_3$	initial init	1	0.402657

Model 2 (Figure 4 B)

Parameter	Description	Starting Value	Finishing Value
k_1	cytokinin ↑ x	1	0.304867
k_2	clv ↓ x	1	5.506337
k_3	rpk2 ↓ x	0	0
k_4	clv ↓ y	0	0
k_5	rpk2 ↓ y	1	3.955426
k_6	x ↑ init	0.1	0.048441
k_7	y ↑ init	0.1	0.209578
p_1	basal x synthesis	0.1	0.025085
p_2	basal y synthesis	0.1	0.0416
p_3	basal init synthesis	.01	0.003168
d_1	x degradation	0.01	0.047735
d_2	y degradation	0.01	0.017703
d_3	init degradation	0.05	0.041424
$base_1$	initial x	0.05	0.452641
$base_2$	initial y	0.05	0.333642
$base_3$	initial init	1	0.351427

Model 3 (Figure 4 C)

Parameter	Description	Starting Value	Finishing Value
k_1	cytokinin ↑ x	1	0.655062
k_2	clv ↓ x	0	0
k_3	rpk2 ↓ x	1	7.480788
k_4	clv ↓ y	1	2.17663
k_5	rpk2 ↓ y	0	0
k_6	x ↑ init	0.1	0.055229
k_7	y ↑ init	0.1	0.27232
p_1	basal x synthesis	0.1	0.014258
p_2	basal y synthesis	0.1	0.015025
p_3	basal init synthesis	.01	0.002324
d_1	x degradation	0.01	0.159216
d_2	y degradation	0.01	0.03027
d_3	init degradation	0.05	0.04435
$base_1$	initial x	0.05	1.239331
$base_2$	initial y	0.05	0.899113
$base_3$	initial init	1	0.540307

Model 4 (Figure 4 D)

Parameter	Description	Starting Value	Finishing Value
k_1	cytokinin ↑ x	1	0.841983
k_2	clv ↓ x	1	2.50779
k_3	rpk2 ↓ x	1	9.162987
k_4	clv ↓ y	0	0
k_5	rpk2 ↓ y	0	0
k_6	x ↑ init	0.1	0.218686
k_7	y ↑ init	0.1	0.070918
p_1	basal x synthesis	0.1	0.009767
p_2	basal y synthesis	0.1	0.004626
p_3	basal init synthesis	.01	0.003158
d_1	x degradation	0.01	0.057663
d_2	y degradation	0.01	0.106677
d_3	init degradation	0.05	0.019892
$base_1$	initial x	0.05	0.072355
$base_2$	initial y	0.05	0.866898
$base_3$	initial init	1	0.740589

Model 5 (Figure 4 E)

Parameter	Description	Starting Value	Finishing Value
k_1	cytokinin ↑ x	1	0.035789
k_2	clv ↓ x	0	0
k_3	rpk2 ↓ x	0	0
k_4	clv ↓ y	1	0.296071

k_5	rpk2 ↓ y	1	6.576975
k_6	x ↑ init	0.1	0.027982
k_7	y ↑ init	0.1	0.359106
p_1	basal x synthesis	0.1	0.004176
p_2	basal y synthesis	0.1	0.03289
p_3	basal init synthesis	.01	0.000394
d_1	x degradation	0.01	0.045523
d_2	y degradation	0.01	0.030657
d_3	init degradation	0.05	0.045014
$base_1$	initial x	0.05	0.551109
$base_2$	initial y	0.05	0.300094
$base_3$	initial init	1	0.702136

Models 6 and 7

Model 6 (CLV inhibits x, Figure 5)

Parameter	**Description**	**Starting Value**	**Finishing Value**
k_1	cytokinin ↑ x	1	0.435963
k_2	clv ↓ x	1	5.048187
k_3	rpk2 ↓ x	0	0
k_4	clv ↓ y	0	0
k_5	rpk2 ↓ y	1	8.082593
k_6	x ↑ init	0.1	0.017249
k_7	y ↑ init	0.1	0.169828
k_8	cytokinin ↓ z	0.5	8.181178
k_9	z ↑ init	0.5	0.768938
p_1	basal x synthesis	0.01	0.004266
p_2	basal y synthesis	0.03	0.023539
p_3	basal init synthesis	.01	0.004809
p_4	basal z synthesis	0.01	0.008215
d_1	x degradation	0.05	0.04629
d_2	y degradation	0.05	0.027294
d_3	init degradation	0.05	0.032801
d_4	z degradation	0.05	0.063203
$base_1$	initial x	1	1.927968
$base_2$	initial y	1	0.232216
$base_3$	initial init	1	0.379397
$base_4$	initial z	1	0.656615

Model 6 (RPK2 inhibits X)

Parameter	**Description**	**Starting Value**	**Finishing Value**
k_1	cytokinin ↑ x	1	0.380677
k_2	clv ↓ x	0	0
k_3	rpk2 ↓ x	1	6.363934
k_4	clv ↓ y	1	2.772667

k_5	rpk2 ↓ y	0	0
k_6	x ↑ init	0.1	0.053368
k_7	y ↑ init	0.1	0.205299
k_8	cytokinin ↓ z	0.5	12.45164
k_9	z ↑ init	0.5	0.854566
p_1	basal x synthesis	0.01	0.059793
p_2	basal y synthesis	0.03	0.032342
p_3	basal init synthesis	.01	0.002267
p_4	basal z synthesis	0.01	0.008643
d_1	x degradation	0.05	0.097205
d_2	y degradation	0.05	0.048109
d_3	init degradation	0.05	0.052553
d_4	z degradation	0.05	0.074966
$base_1$	initial x	1	0.933395
$base_2$	initial y	1	1.584061
$base_3$	initial init	1	0.876901
$base_4$	initial z	1	0.579399

Model 7 (CLV inhibits X, Figure 5)

Parameter	**Description**	**Starting Value**	**Finishing Value**
k_1	cytokinin ↑ x	1	0.863826
k_2	clv ↓ x	1	19.77114
k_3	rpk2 ↓ x	0	0
k_4	clv ↓ y	0	0
k_5	rpk2 ↓ y	1	1.999533
k_6	x ↑ init	0.1	0.040456
k_7	y ↑ init	0.1	0.173769
k_8	cytokinin ↑ z	0.5	1.685863
k_9	z ↓ init	0.5	0.311607
p_1	basal x synthesis	0.01	0.028438
p_2	basal y synthesis	0.03	0.056778
p_3	basal init synthesis	.01	0.004693
p_4	basal z synthesis	0.01	0.005662
d_1	x degradation	0.05	0.014775
d_2	y degradation	0.05	0.018722
d_3	init degradation	0.05	0.038537
d_4	z degradation	0.05	0.118948
$base_1$	initial x	1	0.654166
$base_2$	initial y	1	0.251628
$base_3$	initial init	1	2.202736
$base_4$	initial z	1	0.992124

Model 7 (RPK2 inhibits X)

Parameter	**Description**	**Starting Value**	**Finishing Value**
k_1	cytokinin ↑ x	1	1.463869

k_2	clv ↓ x	0	0
k_3	rpk2 ↓ x	1	19.17415
k_4	clv ↓ y	1	1.013134
k_5	rpk2 ↓ y	0	0
k_6	x ↑ init	0.1	0.027886
k_7	y ↑ init	0.1	0.087528
k_8	cytokinin ↑ z	0.5	2.157959
k_9	z ↓ init	0.5	0.190479
p_1	basal x synthesis	0.01	0.039586
p_2	basal y synthesis	0.03	0.061077
p_3	basal init synthesis	.01	0.00435
p_4	basal z synthesis	0.01	0.012878
d_1	x degradation	0.05	0.012762
d_2	y degradation	0.05	0.024692
d_3	init degradation	0.05	0.055329
d_4	z degradation	0.05	0.042331
$base_1$	initial x	1	0.432841
$base_2$	initial y	1	1.570673
$base_3$	initial init	1	0.574236
$base_4$	initial z	1	0.270798

References

Ashton, N.W. and Cove, D.J. (1977). The isolation and preliminary characterisation of auxotrophic and analogue resistant mutants of the moss, Physcomitrella patens. MGG Mol. Gen. Genet.

Edgar, R.C. (2004). MUSCLE: multiple sequence alignment with high accuracy and high throughput. Nucleic Acids Res. **32**: 1792–1797.

Gordon, S.P., Chickarmane, V.S., Ohno, C., and Meyerowitz, E.M. (2009). Multiple feedback loops through cytokinin signaling control stem cell number within the Arabidopsis shoot meristem. Proc. Natl. Acad. Sci. U. S. A. **106**: 16529–16534.

Hadley, W., Winston, C., Lionel, H., Thomas, Lin, P., Kohske, T., Claus, W., Kara, W., Hiroaki, Y., and Dewey, D. (2016). ggplot2 - Elegant Graphics for Data Analysis (Springer-Verlag New York).

Haeussler, M., Schönig, K., Eckert, H., Eschstruth, A., Mianné, J., Renaud, J.B., Schneider-Maunoury, S., Shkumatava, A., Teboul, L., Kent, J., Joly, J.S., and Concordet, J.P. (2016). Evaluation of off-target and on-target scoring algorithms and integration into the guide RNA selection tool CRISPOR. Genome Biol. **17**: 1–12.

Schaefer, D., Zryd, J.-P., Knight, C.D., and Cove, D.J. (1991). Stable transformation of the moss Physcomitrella patens. Mol. Gen. Genet.: 418–424.

Schindelin, J. et al. (2012). Fiji: An open-source platform for biological-image analysis. Nat. Methods.

Soetaert, K., Petzoldt, T., and Setzer, R.W. (2010). Solving differential equations in R: Package deSolve. J. Stat. Softw.

Strable, J., Wallace, J.G., Unger-Wallace, E., Briggs, S., Bradbury, P.J., Buckler, E.S., and Vollbrecht, E.

(2017). Maize YABBY genes drooping leaf1 and drooping leaf2 regulate plant architecture. Plant Cell.

Team, R.C. (2016). R: A Language and Environment for Statistical Computing. R Found. Stat. Comput.

Whitewoods, C.D. et al. (2018). CLAVATA Was a Genetic Novelty for the Morphological Innovation of 3D Growth in Land Plants. Curr. Biol. **28**: 1–12.